Journal of Sound and Vibration (1977) **50**(4), 533–544

AN EXPERIMENTAL-THEORETICAL CORRELATION STUDY OF NON-LINEAR BENDING AND TORSION DEFORMATIONS OF A CANTILEVER BEAM†

E. H. DOWELL AND J. TRAYBAR

Department of Aerospace and Mechanical Sciences, Princeton University, Princeton, New Jersey 08540, *U.S.A.*

AND

D. H. HODGES

Army Air Mobility Research and Development Laboratory, Moffett Field, California, U.S.A.

(*Received* 21 *June* 1976, *and in revised form* 21 *October* 1976)

An experimental study of the large deformation of a cantilevered beam under a gravity tip load has been made. The beam root is rotated so that the tip load is oriented at various angles with respect to the beam principal axes. Static twist and bending deflections of the tip and bending natural frequencies have been measured as a function of tip load magnitude and orientation. The experimental data are compared with the results of a recently developed non-linear structural theory. Agreement is reasonably good when bending deflections are small compared to the beam span, but systematic differences occur for larger deflections.

1. INTRODUCTION

Hodges and Dowell [1] have formulated a non-linear theory of hingeless rotor blade (cantilever beam) dynamics which indicates that there is an important structural effect on rotor blade stability due to non-linear coupling between elastic flap and chordwise bending and torsion. Flap is bending in the more flexible direction and chordwise that in the stiffer direction. The purpose of the present study has been to devise a simple, non-rotating beam experiment to measure the predicted structural effect and compare the results with theory.

The simplest relevant experiment would appear to be a uniform beam under a static point load. Measurements of the variation of static deflections in flap, chordwise bending and twist, and also flap and chordwise natural frequencies with static load allow an evaluation of the theory. Linear theory would predict a linear variation of flap and chordwise static deflections with load and no twist. Also linear theory would predict no change in natural frequencies with static load. On the other hand, the Hodges-Dowell non-linear theory predicts non-linear variations of static flap, chordwise and twist deflection with static load and a change in natural flap and chordwise natural frequencies with load. Hence, the proposed experiment does provide a critical test of the non-linear theory.

How to provide a static point force to the beam without introducing additional dynamic effects is a delicate question, however. For example, if one uses a weight and gravity to provide the force, its inertial mass would also change directly the dynamic characteristics of the rotor blade. Similarly, for a spring induced static force, dynamic effects are inevitably

† This work was supported by NASA Grant NAS 2-7615, Army Air Mobility and Research Laboratory, Ames Research Center.

introduced as well. In principle for a relatively long, heavy, flexible beam the mass effect may be made as small as desired. Conversely, for a relatively short, stiff beam and a relatively long, soft spring the dynamic effect of the spring may be made as small as desired. In practice neither option leads to beams of convenient dimensions. Hence, we have chosen to use a gravitational force and incorporate the inertial effects of the weight in our mathematical model. The latter, though quantitatively substantial, are nevertheless non-controversial and readily accounted for theoretically. To make the experiment as simple as possible a tip weight was used whose dimensions are small relative to the length of the uniform, rectangular cross-section beam. Hence the torsional frequency is substantially higher (greater than a factor of ten) than either the flap or chordwise frequencies.

In the following, the experimental apparatus and technique are described. Next, the Hodges-Dowell theory is reviewed briefly along with earlier theoretical work, and finally, the experimental data are presented and compared with results from the Hodges-Dowell theory.

2. EXPERIMENTAL APPARATUS AND METHODS

2.1. EXPERIMENTAL APPARATUS

Photographs of the experimental apparatus are shown in Figure 1.

In the experimental phase of the study, beams of various sized rectangular sections were fabricated from 7075 aluminum. Nominal beam dimensions were as follows:

beam no. 1: length (radius) 20 in, width 1 in, thickness $\frac{1}{8}$ in;
beam no. 2: length (radius 20 in, width $\frac{1}{2}$ in, thickness $\frac{1}{8}$ in;
beam no. 3: length (radius) 30 in, width $\frac{1}{2}$ in, thickness $\frac{1}{8}$ in.

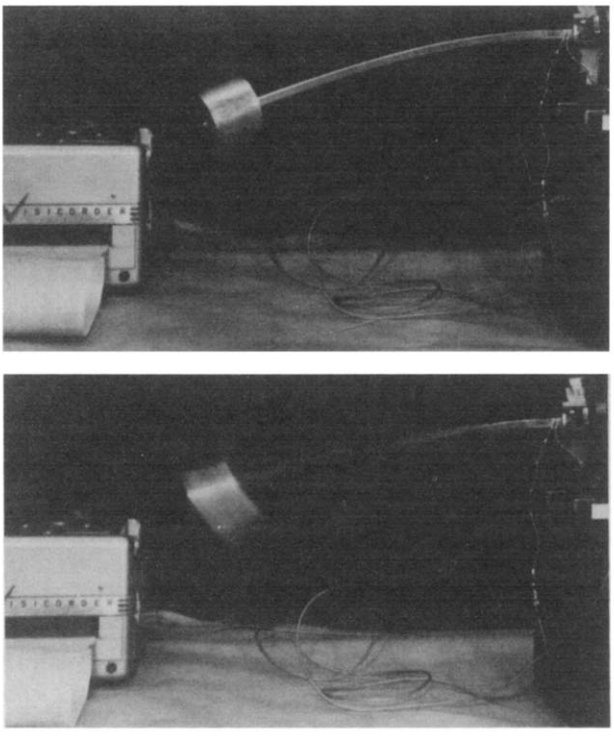

Figure 1. Photograph of apparatus for frequency measurements showing steady and oscillating conditions.

Beams 2 and 3 were instrumented with strain gages mounted at the roots on the width and thickness portions of the beam to measure flap and chordwise beam natural frequencies. Beam tip-end static deflection was measured as well as natural frequency. For these measurements, a simple projection on graph paper was made of the beam tip-end elastic axis and leading edge points as a function of applied load and pitch angle.

All beams were end mounted in specially fabricated end fixtures that ensured positive support and clamping. These beam end-fixtures were inserted into a milling machine type, precision, indexing-chuck that provided both a secure, stable mount and the accurate, repeatable angular settings required.

2.2. EXPERIMENTAL METHODS

Various experiments were conducted with the previously described beam specimens and apparatus. The principal parameters varied included blade tip load (P) and blade pitch angle (θ). Figure 2 is a schematic showing typical loading procedures and excitation/deflection sense.

In the static deflection experiments, the selected values of pitch angle (measured at the blade root end) were pre-set and locked for each run. A weight bucket was attached to a small machine screw (by a string) at the blade tip elastic axis point. Then, increasing loads in $\frac{1}{2}$ pound increments were applied and the beam tip elastic-axis and leading points was projected on graph paper.

In the natural frequency experiments, selected tip loads were applied (as shown schematically in Figure 2) and the beam natural frequencies were measured as functions of beam pitch angle (measured at the beam root end) and excitation sense. Each tip weight was rigidly attached to the beam tip end and the beam was excited in flapwise as well as chordwise senses (see Figure 2). Strain gages used as frequency transducers and their associated instrumentation permitted relatively accurate measurement of both the flapwise and chordwise frequencies. The determination of flapwise and chordwise frequencies was done in separate experiments. That is, the weight mounted at the tip-end was excited (by hand) in the flapwise sense so that

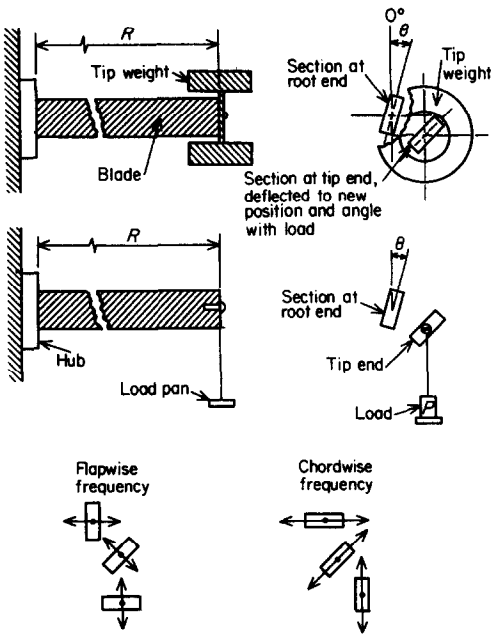

Figure 2. Schematic showing typical loading procedures and excitation/deflection sense.

the output trace of frequency in the flapwise sense was of acceptable amplitude, whereas the output trace in the chordwise sense was minimized. The same experiment was then repeated except that the beam was now excited in the chordwise sense with the flapwise motion minimized.

For additional detail concerning the experiment, see reference [2]. All data obtained are presented there in tabular form.

3. THEORETICAL MODEL

Hodges and Dowell [1] have developed non-linear equations of motion for the elastic bending and torsion of twisted non-uniform rotor blades (rotating cantilever beams). The equations are valid to second order in that squares of bending slopes, torsion deformation, chord/length and thickness/length ratios are neglected with respect to unity. Thus, only the most important non-linear terms are retained in the equations. Although there have been other equations developed for rotor blade applications [3–5] the Hodges-Dowell equations have the structural and inertial non-linear terms correct to second order for a fully elastic blade. Solutions to these equations for rotor blade applications have been obtained by Hodges and Ormiston [6, 7] using the Galerkin method. Results indicate that both structural and inertial non-linearities are very important in analyzing the stability of hingeless rotor blades. Here, only the structural non-linearities are considered.

For a non-rotating uniform, untwisted beam without offsets between the elastic, center of mass, and tension axes, the equations of motion may be written, to second order, as

$$EI_2 v'''' + (EI_2 - EI_1)(\phi w'')'' + m\ddot{v} + I_v = P\delta(R-x)\cos\theta + mg\cos\theta,$$

$$(EI_2 - EI_1)(\phi v'')'' + EI_1 w'''' + m\ddot{w} + I_w = P\delta(R-x)\sin\theta + mg\sin\theta,$$

$$-GJ\phi'' + (EI_2 - EI_1)v''w'' + mk_m^2\ddot{\phi} + I_\phi = 0, \tag{1}$$

where I_v, I_w and I_ϕ are the dynamic contributions of a tip weight of mass $M_{TIP} = P/g$ with center of mass at $x = R$. The bending stiffness constants are EI_1 and EI_2, and the torsion stiffness constant GJ. The chordwise and flap bending deflections are v and w, respectively (see Figure 3), and the torsion deflection is ϕ [1]. Note that ϕ is measured with respect to the

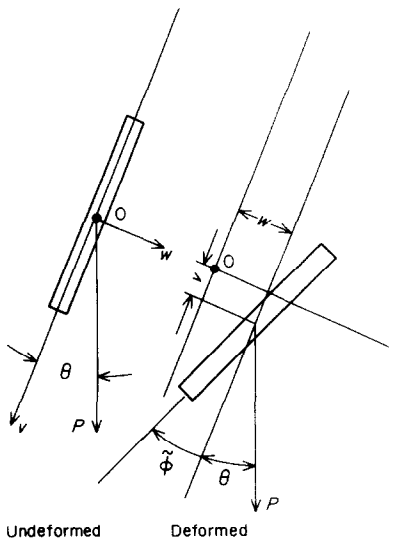

Figure 3. Beam cross-section (end view); undeformed and deformed O is common point.

deformed elastic axis. Equation (1) has been derived by Hamilton's Principle (without the tip weight) in reference [1]. Also shown in Figure 3 is the geometric twist angle $\tilde{\phi} = \phi + \int_0^x v' w'' \, dx$. See section 4 for the physical meaning of $\tilde{\phi}$. (Also a list of symbols, for reference, is given in the Appendix.)

For determining dynamic stability of a rotor blade under the influence of aerodynamic loads, the angle $\tilde{\phi}$ is generally approximated as ϕ in the structural terms, but not in the aerodynamic terms [6, 7]. However, for static instability at $\theta = 0$ (lateral buckling) Hodges and Peters [8] have shown that including the geometric effect, the integral in the expression for $\tilde{\phi}$, in the structural terms can change the lateral buckling load modestly. Since equation (1) does not contain this effect we should expect a small error in lateral buckling load prediction [8]. More significantly, since the theory ignores v'^2, w'^2 and ϕ^2 with respect to unity, we should observe a deterioration of the accuracy of the theory when the largest of these quantities (in our case w'^2) is no longer small with respect to unity.

The major static loading effect from the tip weight is represented here as a point load by a Dirac delta function times the magnitude P of the tip weight. The tip weight is assumed to be a flat disc of diameter D and thickness l. Thus, the kinetic energy from the tip weight motion is

$$T_M = \frac{1}{2}\frac{P}{g}\left[\dot{v}^2 + \dot{w}^2 + \frac{D^2}{8}\dot{\phi}^2 + \left(\frac{3D^2 + 4l^2}{48}\right)(\dot{v}'^2 + \dot{w}'^2)\right]_{\bar{x}=R}. \tag{2}$$

From T_M, the inertial terms I_v, I_w and I_ϕ may be deduced by variational methods. Alternatively, one may substitute assumed mode shape functions into equation (2) and equation (1) to obtain ordinary differential equations in terms of generalized co-ordinates without explicitly writing I_v, I_w and I_ϕ. Standard non-rotating cantilever beam normal mode shape functions are used in all theoretical calculations in this paper. Thus

$$\bar{v} = \sum_{j=1}^{N} V_j(\tau)\,\psi_j(\bar{x}), \qquad \bar{w} = \sum_{j=1}^{N} W_j(\tau)\,\psi_j(\bar{x}), \qquad \phi = \sum_{j=1}^{N} \Phi_j(\tau)\,\Theta_j(\bar{x}), \tag{3}$$

where $(\bar{\ })$ indicates non-dimensionalization with respect to the beam span, R, τ is dimensionless time $t\sqrt{(g/R)}$, and

$$\psi_j = \cosh(\beta_j \bar{x}) - \cos(\beta_j \bar{x}) - \alpha_j[\sinh(\beta_j \bar{x}) - \sin(\beta_j \bar{x})], \qquad \Theta_j = \sqrt{2}\sin(\gamma_j \bar{x}). \tag{4}$$

The constants α_j and β_j are tabulated in reference [9] and γ_j is given by $\pi(j - \frac{1}{2})$. Letting

$$V_j = V_{0j} + \Delta V_j(\tau), \qquad W_j = W_{0j} + \Delta W_j(\tau), \qquad \Phi_j = \Phi_{0j} + \Delta\Phi_j(\tau), \tag{5}$$

one may obtain two sets of equations—one for the static equilibrium position of the beam and the other for (small perturbation) motions about that equilibrium. The equilibrium equations consist of $3N$ non-linear algebraic equations in V_{0j}, W_{0j} and Φ_{0j} which are solved by iteration using the Newton-Raphson method. The dynamic equations may be linearized for small motions about the equilibrium shape. They then become $3N$ linear constant coefficient ordinary differential equations in ΔV_j, ΔW_j and $\Delta\Phi_j$, solvable with a standard eigenvalue algorithm. The coefficients are functions of V_{0j}, W_{0j} and Φ_{0j}. The equilibrium equations are

$$\sum_{j=1}^{N}\left[A\beta_j^4\delta_{ij}V_{0j} + (A-B)\sum_{k=1}^{N}K_{jki}\Phi_{0j}W_{0k}\right] = 2\bar{P}\cos\theta(-1)^{i+1} + A_i\cos\theta,$$

$$\sum_{j=1}^{N}\left[(A-B)\sum_{k=1}^{N}K_{jki}\Phi_{0j}V_{0k} + B\beta_j^4\delta_{ij}W_{0j}\right] = 2\bar{P}\sin\theta(-1)^{i+1} + A_i\sin\theta,$$

$$\sum_{j=1}^{N}\left[C\gamma_j^2\delta_{ij}\Phi_{0j} + (A-B)\sum_{k=1}^{N}K_{ijk}V_{0j}W_{0k}\right] = 0, \qquad i = 1, 2, \ldots, N, \tag{6}$$

where

$$A = EI_2/mgR^3, \qquad B = EI_1/mgR^3, \qquad C = GJ/mgR^3, \qquad \bar{P} = P/mgR,$$

$$A_i = \int_0^1 \psi_i \, d\bar{x}, \qquad K_{ijk} = \int_0^1 \Theta_i \psi_j'' \psi_k'' \, d\bar{x}, \qquad \delta_{ij} = \text{Kronecker delta.} \tag{7}$$

The perturbation equations may be expressed as a matrix equation from which natural frequencies may be calculated in the usual way,

$$[M]\{\dot{X}\} + [K]\{X\} = 0, \tag{8}$$

where $[M]$ is the mass matrix, $[K]$ is the stiffness matrix, and

$$\{X\} = \begin{Bmatrix} \Delta V_i \\ \Delta W_i \\ \Delta \Phi_i \end{Bmatrix}, \tag{9}$$

$$[M] = \begin{bmatrix} \delta_{ij} + \bar{P}(B_{ij} + \alpha C_{ij}) & 0 & 0 \\ 0 & \delta_{ij} + \bar{P}(B_{ij} + \alpha C_{ij}) & 0 \\ 0 & 0 & \bar{k}_m^2 \delta_{ij} + \bar{P}\dfrac{\bar{D}^2}{4}(-1)^{i+1} \end{bmatrix}, \tag{10}$$

$$[K] = \begin{bmatrix} A\beta_j^4 \delta_{ij} & (A-B)\sum_{k=1}^{N} K_{kji}\Phi_{0k} & (A-B)\sum_{k=1}^{N} K_{jki} W_{0k} \\ (A-B)\sum_{k=1}^{N} K_{kji}\Phi_{0k} & B\beta_j^4 \delta_{ij} & (A-B)\sum_{k=1}^{N} K_{jki} V_{0k} \\ (A-B)\sum_{k=1}^{N} K_{ijk} W_{0k} & (A-B)\sum_{k=1}^{N} K_{ijk} V_{0k} & C\gamma^2 \delta_{ij} \end{bmatrix}, \tag{11}$$

where

$$B_{ij} = \psi_i \psi_j|_{\bar{x}=1} = 4(-1)^{i+j}, \qquad C_{ij} = \psi_i^* \psi_j^*|_{\bar{x}=1} = 4(-1)^{i+j}\alpha_i \alpha_j \beta_i \beta_j, \qquad \bar{D} = D/R,$$

$$\alpha = (3\bar{D}^2 + 4\bar{l}^2)/48, \qquad \bar{l} = l/R, \qquad \bar{k}_m = k_m/R. \tag{12}$$

For additional details of the calculation procedure, see references [6] and [7].

4. EXPERIMENTAL RESULTS AND COMPARISON WITH THEORY

4.1. STATIC DEFLECTIONS

Results were obtained for two beams, one of $\frac{1}{2}$ in $\times$ $\frac{1}{8}$ in cross-section, the other of 1 in $\times$ $\frac{1}{8}$ in, and both 20 in in length [2]. The data discussed below are for the former. The static experimental loading is a simple tip weight with the beam rotated to achieve various loading angles. Measurements of flap and chordwise bending deflection at the beam (free end) tip, W_{TIP} and V_{TIP}, as well as twist, $\tilde{\phi}_{\text{TIP}}$, have been obtained for $\theta = 0° \to 90°$ and for $P = 0 \to 5\#$. $\tilde{\phi}$ is the angle determined by the projection of the elastic axis and leading edge of the cross-section at the beam tip on a plane perpendicular to the undeformed cross-section. Intermediate values of W, V and $\tilde{\phi}$ along the beam span were also obtained [2].

The most sensitive indicator of the difference between the linear and non-linear theoretical models is the twist as it is identically zero in the linear model. Theoretical results are for the non-linear model unless otherwise stated. In Figures 4(a)–(e) results for static tip twist are presented for various loading angles, θ, as a function of the magnitude of the load, P. For

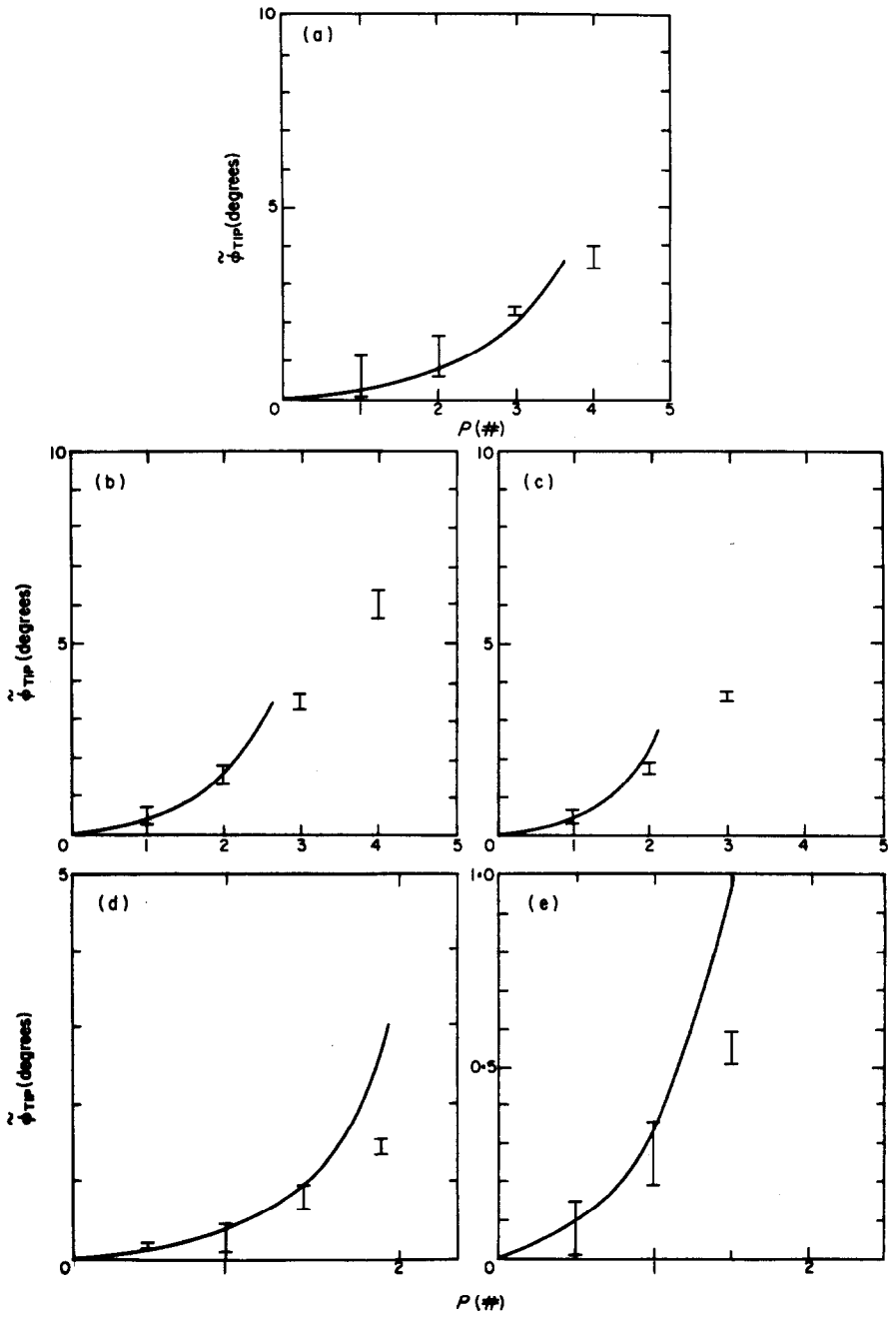

Figure 4. Static twist *vs.* load. (a) $\theta = 15°$; (b) $\theta = 30°$; (c) $\theta = 45°$; (d) $\theta = 60°$; (e) $\theta = 75°$. ——, Theory. I, experiment.

$\theta = 0°$ and 90° theory predicts no twist and, within the accuracy of the experimental measurement, there was none. There is reasonable agreement for any θ and sufficiently small P (and hence $\tilde{\phi}$). As θ increases, the range of P for which there is reasonable agreement becomes smaller. This is thought to be associated with the larger static flap deflections (for a given P) as $\theta \to 90°$. In the Hodges-Dowell theory, terms of the order of the square of the flap deflection, w, divided by beam span R, are neglected with respect to unity [1].

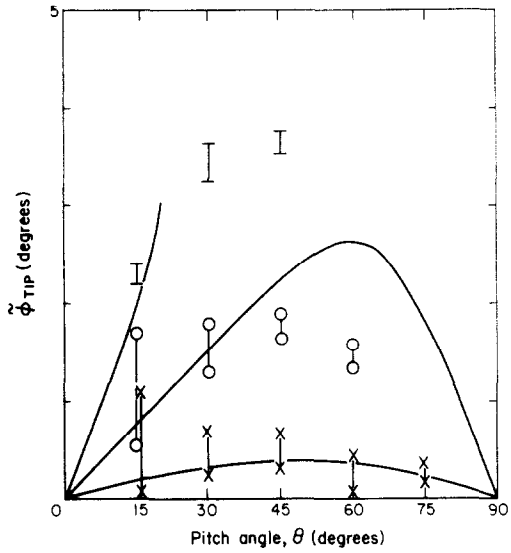

Figure 5. Static twist *vs.* pitch angle; various loads. ——, Theory. Experiment: I, $P = 3\#$; ⟟, $P = 2\#$; ⟟, $P = 1\#$.

A cross-plot of the data in terms of $\tilde{\phi}$ *versus* θ for various P is given in Figure 5. In Figures 6 and 7, the flap and chordwise tip deflections are plotted in the same format. As mentioned above, for large P, say $P \geqslant 3\#$, and $\theta \to 90°$, the flap deflections are such that $(w/R)^2$ is no longer negligible compared to unity. Where the theoretical curves are terminated, the theoretical Newton-Raphson solution procedure failed to converge or there was a change in sign of $\tilde{\phi}$ or V_{TIP}, indicating a jump from one equilibrium configuration to another. Again, this occurs for large $(w/R)^2$ and the theoretical results under such conditions cannot be regarded as reliable. Multi-mode calculations were carried out using the Newton-Raphson method to ensure *modal* convergence. Five modes for each of flapwise, chordwise and twist deflections were used to achieve well-converged modal solutions.

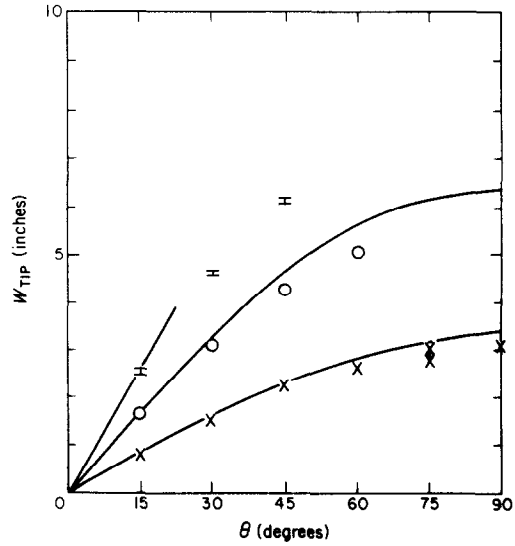

Figure 6. Static flap deflection *vs.* pitch angle; various loads. ——, Theory. Experiment: I, $P = 3\#$; ⟟, $P = 2\#$, ⟟, $P = 1\#$.

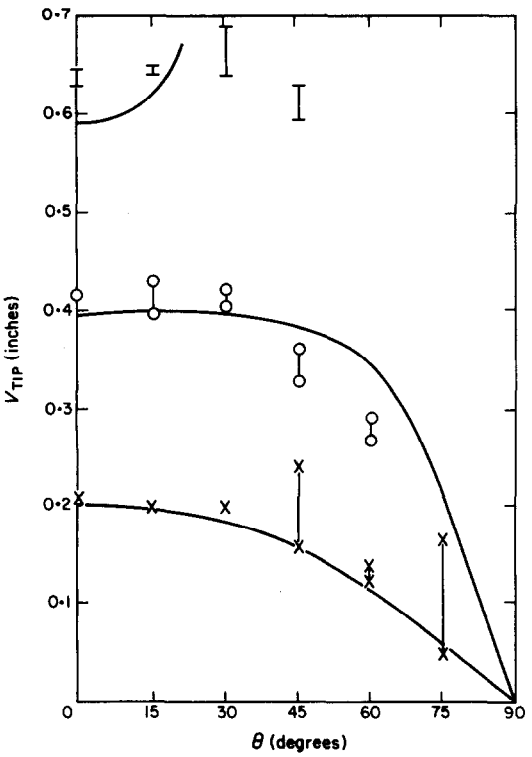

Figure 7. Static lag or chordwise deflection *vs.* pitch angle; various loads. ——, Theory. Experiment: I, $P = 3\#$; ⟆, $P = 2\#$; ⟆, $P = 1\#$.

4.2. NATURAL FREQUENCIES

Results were obtained for two beams, one 20 in long and the other 30 in, and both of cross-section $\frac{1}{2}$ in × $\frac{1}{8}$ in [2]. The data discussed below are for the former. Measurements of flap and lag frequencies have been obtained for $\theta = 0° \rightarrow 90°$ and P up to $10\#$ for $\theta = 0°$ [2]. In Figures 8(a)–(d) experimental results are shown for $P = 1$ and $2\ \#$ over a range of θ. Non-linear theoretical results for the same conditions are also shown. Linear theory would predict no change in frequency with θ (the lag results being those for $\theta = 0°$ and the flap results those for $\theta = 90°$). The dead weight load *per se* has (theoretically) no effect on the flapwise mode for $\theta = 90°$ or the chordwise mode for $\theta = 0°$. The weight still contributes a dynamic mass effect, of course.

The trends of the theoretical and experimental data are broadly similar for $P = 1\#$. However, systematic deviations occur for $P = 2\#$, particularly in the flap mode. This is attributed to the static flap deflection becoming a significant fraction of beam span under these conditions.

It is of interest to examine the special case $\theta = 0°$ for large P. For $\theta = 0°$, no static flap deflection will occur until the beam laterally buckles. The buckling load is that value of P for which the flap frequency goes to zero. The pre-buckling static lag deflection is always small compared to the beam span and hence well satisfies the assumptions of the non-linear theory. Experimental as well as linear and non-linear theoretical results are shown in Figure 9. *Linear theory is in poor agreement* with the experimental data for large tip weights and, in particular, does not predict any buckling at all. In the linear model, the decrease in flap frequency is solely due to the *mass* of the tip weight. *On the other hand,* the non-linear theory is in good agreement with the experimental data up to and including the buckling load. Also

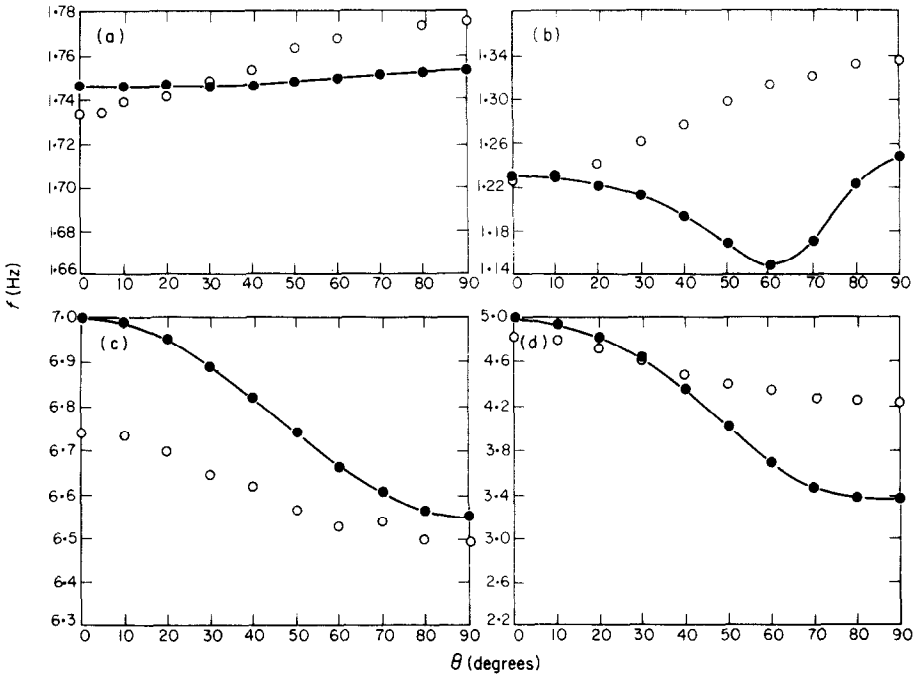

Figure 8. Flap frequency *vs.* pitch angle. (a) $P = 1\#$; (b) $P = 2\#$, lag frequency *vs.* pitch angle; (c) $P = 1\#$; (d) $P = 2\#$. o, Experiment; —●—, theory.

shown for reference is the buckling load calculated from the more accurate Hodges-Peters theory [8].†

Results were also obtained for the chordwise frequency; there were no systematic differences, for the range of parameters studied, among the linear and non-linear theoretical results and experimental results [2] for $\theta = 0°$.

In all theoretical calculations the following beam parameters were used:

$E = 10{\cdot}576 \times 10^6$ lb/in^2, $G = 4{\cdot}0383 \times 10^6$ lb/in^2, $\nu = 0{\cdot}31$, $\rho = 0{\cdot}1014\#/\text{in}^3$;
$I_1, I_2 = ct^3/12, tc^3/12, J = 0{\cdot}2807ct^3$, where $c = 0{\cdot}4999$ in, $t = 0{\cdot}1251$ in and $R = 19{\cdot}985$ in.

The values of c, t, R and ρ were measured directly. The values of I_1, I_2 and J are the accepted theoretical values in terms of c and t. The values of E, G and ν, although close to the usual "handbook values", were determined as follows: E was inferred by requiring the theoretical and experimental values of flap bending frequency to be equal for the unloaded beam. G was inferred by requiring the theoretical (Hodges-Peters [8]) and experimental lateral buckling loads to be equal. ν was calculated from $G = E/2(1 + \nu)$. However, it should be noted that even if one used instead the accepted "handbook" values of $E = 10{\cdot}5 \times 10^6$ lb/in^2 and $\nu = 0{\cdot}3$–$0{\cdot}33$ there would be little change in the theoretical results.

As an independent check on the beam parameters employed, the torsional frequency of the beam was measured and compared to the value calculated by using the above parameters. The results were as follows:

experimental, $\omega_{\text{TORSION}} = 673{\cdot}9$ Hz;
theoretical, $\omega_{\text{TORSION}} = 688$ Hz.

The agreement is within approximately 2%.

† Corrected for non-zero warping rigidity [10].

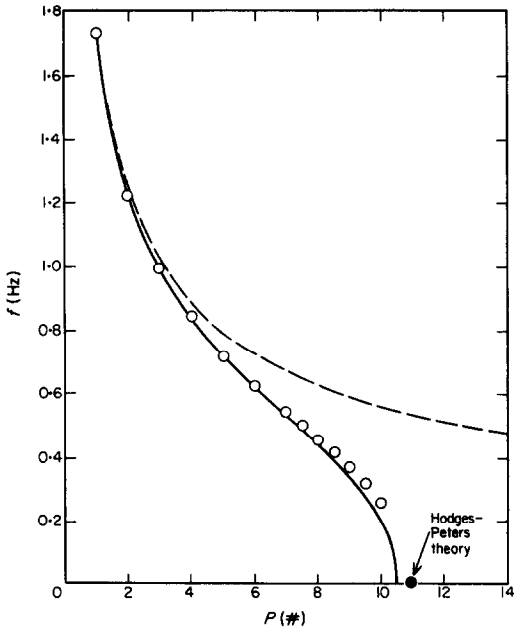

Figure 9. Flap frequency *vs.* load; $\theta = 0°$. ○, Experiment; ---, linear theory; ——, non-linear theory.

5. CONCLUDING REMARKS

From the correlation of theory and experiment, we see there is reasonably good agreement for the linear and *initial* non-linear behavior. As the tip deflections reach a significant fraction of beam span, there are systematic differences between theory and experiment. This is consistent with the basic assumption of the Hodges-Dowell theory in which squares of bending slopes are neglected compared to one.

ACKNOWLEDGMENT

The authors would like to thank Dr R. A. Ormiston and Dr D. A. Peters for several helpful discussions of this work.

REFERENCES

1. D. H. Hodges and E. H. Dowell 1974 *NASA TN D*-7818. Non-linear equations of motion for the elastic bending and torsion of twisted non-uniform rotor blades.
2. E. H. Dowell and J. Traybar 1975 (January and December) *Princeton University, AMS Reports No.* 1194 and 1257. An experimental study of the non-linear stiffness of a rotor blade undergoing flap, lag and twist deformations.
3. M. L. Mil' *et al.* 1967 *NASA TT F*-494, 430–432. Helicopters: Calculation and design, Volume I, Aerodynamics.
4. P. J. Arcidiacono 1969 (February) *USAAVLABS TR*68-18*A*, Vol. I. Steady flight differential equations of motion for a flexible helicopter blade with chordwise mass unbalance.
5. P. Friedmann and P. Tong 1972 *NASA CR*-114485. Dynamic non-linear elastic stability of helicopter rotor blades in hover and in forward flight.
6. D. H. Hodges and R. A. Ormiston 1973 *American Institute of Aeronautics and Astronautics Paper No.* 73-405. Stability of elastic bending and torsion of uniform cantilevered rotor blades in hover.
7. D. H. Hodges and R. A. Ormiston 1975 *NASA TN D*-8192. Stability of elastic bending and torsion of uniform cantilevered rotor blades in hover with variable structural coupling.

8. D. H. HODGES and D. A. PETERS 1975 *International Journal of Solids and Structures* **II**, 1269–1280. On the lateral buckling of uniform slender cantilever beams.
9. TISH-CHUN CHANG and R. R. CRAIG 1969 *Engineering Mechanics Research Laboratory Circular* 1068, *University of Texas, Austin*. On normal modes of uniform beams.
10. S. P. TIMOSHENKO and J. M. GERE 1961 *Theory of Elastic Stability*. New York: McGraw-Hill Book Company, Inc., second edition, see pp. 259–261.

APPENDIX: LIST OF SYMBOLS

A, B, C	dimensionless bending and tension stiffness constants
A_i–K_{ijk}	Galerkin integrals
c	beam width
E	modulus of elasticity
f	frequency
G	shear modulus
g	gravitational constant
I_1, I_2	flap, chordwise area moments; $ct^3/12$, $tc^3/12$
I_v, I_w, I_ϕ	symbolic notation for dynamic contributions of the tip weight
J	torsion stiffness constant, $0{\cdot}2807ct^3$ for $t/c \cong 1/4$
k_m	beam mass radius of gyration
$[k]$	stiffness matrix
$[M]$	mass matrix
M_{TIP}	tip mass
P	gravity tip load; $=M_{\text{TIP}}g$
R	beam span
t	beam thickness
T_M	kinetic energy of tip weight motion
v	chordwise bending deflection; also called lag
w	flap bending deflection perpendicular to v
V_j, W_j, ϕ_j	generalized co-ordinates for bending and torsion
x	position co-ordinate along beam span
$\bar{x}$	$=x/R$
α	tip weight inertia
δ_{ij}	Kronecker delta
δ	Dirac delta function
$\Delta( )$	perturbation quantity
ϕ	twist about deformed elastic axis
$\tilde{\phi}$	projected twist angle (see section 4)
θ	angle between beam chord and vertical (pitch angle) at beam root
m	beam mass per unit length
$(^-)$	dimensionless variable, with respect to R for lengths and mgR for weight
$( )_0$	equilibrium quantity
$( )'$	derivative with respect to x
$( )^*$	derivative with respect to $\bar{x}$